HHS Public Access

Author manuscript

Nat Commun. Author manuscript; available in PMC 2014 December 11.

Published in final edited form as:

Nat Commun. ; 5: 3984. doi:10.1038/ncomms4984.

Haemodynamic and extracellular matrix cues regulate the mechanical phenotype and stiffness of aortic endothelial cells

Caitlin Collins[1], **Lukas D. Osborne**[2], **Christophe Guilluy**[1], **Zhongming Chen**[1], **E Tim O'Brien III**[2], **John S. Reader**[1], **Keith Burridge**[1,3,4], **Richard Superfine**[2], and **Ellie Tzima**[1,3,4]

[1]Department of Cell Biology and Physiology, University of North Carolina at Chapel Hill, Chapel Hill, NC 27599

[2]Department of Physics and Astronomy, University of North Carolina at Chapel Hill, Chapel Hill, NC 27599

[3]Lineberger Cancer Center, University of North Carolina at Chapel Hill, Chapel Hill, NC 27599

[4]McAllister Heart Institute, University of North Carolina at Chapel Hill, Chapel Hill, NC 27599

Abstract

Endothelial cell (ECs) lining blood vessels express many mechanosensors, including platelet endothelial cell adhesion molecule-1 (PECAM-1), that convert mechanical force to biochemical signals. While it is accepted that mechanical stresses and the mechanical properties of ECs regulate vessel health, the relationship between force and biological response remains elusive. Here we show that ECs integrate mechanical forces and extracellular matrix (ECM) cues to modulate their own mechanical properties. We demonstrate that the ECM influences EC response to tension on PECAM-1. ECs adherent on collagen display divergent stiffening and focal adhesion growth compared to ECs on fibronectin. This is due to PKA-dependent serine phosphorylation and inactivation of RhoA. PKA signaling regulates focal adhesion dynamics and EC compliance in response to shear stress *in vitro* and *in vivo*. Our study identifies a ECM-specific, mechanosensitive signaling pathway that regulates EC compliance and may serve as an atheroprotective mechanism maintains blood vessel integrity *in vivo*.

Introduction

Mechanical forces influence nearly all aspects of cell behaviour, including apoptosis, transcription and translation, differentiation and cell migration[1, 2, 3, 4, 5]. The mechanical environment of a cell consists of both cell-generated (endogenous) and applied (exogenous)

Corresponding Author: Ellie Tzima, Department of Cell Biology and Physiology, 6335 MBRB, CB 7545, 111 Mason Farm Rd. Chapel Hill, NC 27599, etzima@med.unc.edu, 919-843-9455.

Author Contributions:

C.C. and E.T. designed the experiments. C.C., L.D.O., and C.G. performed the experiments and analyzed data. Z.C., E.T.O., J.S.R., R.S., and K.B. helped with experimental design and procedures. C.C. and E.T. wrote the manuscript and all authors provided detailed comments.

Competing financial interest. The authors declare no competing financial interests.

forces. Endogenous forces are generated when a cell pulls on the ECM or its neighbours via its cytoskeleton. Examples of exogenous forces include the mechanical force of shear stress applied on ECs due to blood flow, as well as the stretching of vascular cells due to blood pressure. It is now well accepted that mechanical stresses determine the mechanical properties of cells, which, in turn, influence cell function in both physiology and disease. Nevertheless, the relationship between force and biological response remains elusive.

Various methods have been used to apply exogenous forces to cells[6, 7, 8]. These studies have revealed that when force is applied to mechanosensitive proteins, cells respond by increasing their stiffness. This is a physiological response that is required in order to resist the applied force; however, increased stiffness is also associated with pathologies such as cardiovascular disease and cancer[9, 10, 11] We and others have demonstrated that the stiffening response requires the coordination of numerous signaling cascades, including activation of the small GTPase RhoA[6, 7, 12]. Effectors downstream of the GTPase coordinate changes in the actin cytoskeleton and focal adhesions in an effort resist the applied force[12].

While much work has focused on integrin-mediated force transduction, recent work has highlighted other mechanosensitive proteins, such as cadherins and PECAM-1[5, 12, 13, 14]. PECAM-1 functions as a mechanosensor in the endothelium and activates a number of intracellular signaling cascades in response to the haemodynamic force of shear stress[15]. We recently reported that ECs adherent on fibronectin (FN) generate an adaptive stiffening response when tension is applied to PECAM-1[12], and this response is dependent on integrin ligation with the underlying ECM. Integrin heterodimers differ in their ECM specificity based on their α/β subunit composition and therefore bind to distinct ECM proteins. Several studies have reported matrix-specific signaling through different integrin subtypes within the endothelium[16, 17, 18]. Throughout most of the vasculature, collagen (CL) and laminins are the predominant ECM proteins. However, distinct regions of the vasculature are rich in FN deposition and therefore differ in matrix composition. Variances in matrix composition along blood vessels permit activation of ECM-specific signaling cascades in localized regions of the vasculature. For instance, fluid shear stress activates protein kinase A (PKA) in ECs adherent on CL, whereas PKA activity is unaffected when ECs adherent on FN are exposed to shear stress[18]. While ECM-specific signaling cascades have been identified, how these divergent signaling pathways affect mechanical signaling, cell mechanics, and cellular functions are not understood.

Here we investigate how the ECM identity and signaling through discrete integrin subtypes influences the cellular response to tension on PECAM-1. We reveal that the ECM composition has a profound effect on EC stiffness, both *in vitro* and *in vivo* in the haemodynamic environment of the vessel. We identify that CL-dependent and $G\alpha_s$-mediated activation of PKA in response to mechanical force on PECAM-1 negatively regulates RhoA activity. Furthermore, we show that PKA-mediated inhibition of RhoA modulates the EC force response and focal adhesion dynamics *in vitro* and *in vivo* to, ultimately, dampen EC stiffness in the CL-rich descending aorta.

Results

The ECM determines the mechano-response to force on PECAM-1

In order to investigate the role of ECM composition on the mechanical response to tension on PECAM-1, we utilized magnetic tweezers to apply pulsatile force to ECs adherent on FN or CL. ECs incubated with anti-PECAM-1-coated paramagnetic beads were subjected to 2-second pulses of force over a 2-minute time course (Fig. 1a). In ECs adherent on FN, application of successive pulses of force on PECAM-1 resulted in a significant decrease in bead displacement during latter pulses (Fig. 1b). This observed reduction in bead displacement is indicative of adaptive stiffening and consistent with previous work[12]. Surprisingly, when ECs adherent on CL were stimulated with the identical force regimen, we could not detect a significant change in pulse-to-pulse bead displacement, suggesting that the cells do not generate a force response in this context (Fig. 1b). Absolute displacement of anti-PECAM-1 coated beads during the first pulse of force was nearly identical on both FN and CL (Supplementary Fig. 1). These results indicate that ECs adherent on FN or CL differ dramatically in their ability to respond to exogenous force application.

Work from our group and others has demonstrated that the adaptive cellular stiffening response is mediated, in part, by an increase in focal adhesions that function to resist the applied force[12, 19]. We assessed the focal adhesion profile in ECs plated on FN and CL before and after force manipulation. As previously reported, ECs adherent on FN exhibited robust focal adhesion growth in response to force on PECAM-1 (Fig. 1c). Conversely, and in agreement with the magnetic tweezers data, focal adhesion size or number did not significantly increase in ECs adherent on CL following force application. Taken together, these data indicate that the ECM composition has a profound effect on the cellular response to tension on PECAM-1. ECs adherent on FN generate an adaptive stiffening response, accompanied by significant focal adhesion growth, whereas ECs adherent on CL do not generate a significant force response or restructure focal adhesions in response to tension on PECAM-1.

Phosphoinositide 3-kinase (PI3K) is a critical regulator of PECAM-1-mediated adaptive stiffening on FN by allowing integrin activation and downstream activation of RhoA[12]. In order to examine PI3K activation in ECs adherent on CL, anti-PECAM-1-coated paramagnetic beads bound to ECs expressing a GFP-PH fusion protein (which serves as a sensor for PI3-lipids) were subjected to force using a permanent ceramic magnet. Brief force application induced rapid PI3K activation around anti-PECAM-1-coated beads (Supplementary Fig. 2a) at levels similar to those previously reported in ECs adherent on FN[12]. These results suggest that the impaired mechanical response on CL is not due to insufficient PI3K activation. In order to assess force-dependent changes in collagen-binding integrin ($\alpha 2\beta 1$) activity, ECs adherent on CL were subjected to force and immunostained with an antibody that recognizes ligated $\beta 1$ integrins. ECs exhibited transient but robust integrin activation after force application (Supplementary Fig. 2b), suggesting that the lack of a mechanical response in ECs adherent on CL may be due to divergent signaling downstream of CL-binding integrins.

The ECM regulates mechanosensitive PKA and RhoA activation

Activation of the small GTPase RhoA is known to be important for the cellular stiffening response[6, 7, 12]. Importantly, RhoA activation in response to tension on PECAM-1 requires integrin activation and ligation with the underlying ECM[12]. Although cells on CL exhibited significant integrin activation in response to tensional force on PECAM-1, we wanted to evaluate if downstream RhoA activation was affected by ECM composition. Tension on PECAM-1 resulted in robust, but transient activation of RhoA, as levels of GTP-bound RhoA increased at 5 min of force, but returned to basal levels by 30 min of force (Fig. 2a). This transient response is in striking contrast to the prolonged RhoA activation that occurs when tension is applied to ECs adherent on FN (Fig. 2b).

PKA has been implicated as a negative regulator of RhoA activity. The kinase can phosphorylate RhoA at serine 188[20], and phosphorylation of this residue promotes association of the GTPase with guanine dissociation inhibitor (GDI). ECs exhibit mechanosensitive and matrix-specific activation of PKA, such that the kinase is activated in ECs adherent on CL in response to the mechanical stimulus of fluid shear stress but not activated in ECs adherent on FN[18]. Thus, we hypothesized that PKA may be differentially regulated in response to tension on PECAM-1, depending on the identity of the underlying ECM. In agreement with our hypothesis, when tension was applied to PECAM-1 on cells adherent to CL, we observed a significant force-dependent increase in PKA phosphorylation (Fig. 2c). However, we did not detect a significant change in PKA activity when cells on FN were subjected to force (Fig. 2d). In further support of matrix-specific activation of PKA, we also detected CL-specific activation of the downstream transcription factor cAMP-response element binding protein (CREB), while CREB phosphorylation levels did not change in cells adherent on FN (Fig. 2e,f).

PKA activation is mediated by $G\alpha_s$-dependent signaling

PKA exists as a holoenzyme that comprises two regulatory subunits bound to two catalytic subunits. Under low levels of cAMP, the regulatory subunits remain intact and holds the holoenzyme inactive. However, when the intracellular cAMP concentration increases, the nucleotide binds the regulatory subunits and releases the active catalytic subunits. We assessed whether mechanical tension on PECAM-1 results in increased cAMP levels and examined the role of the ECM in this activation. Consistent with our PKA data, we detected a significant force-dependent increase in cAMP levels in ECs adherent to CL, while levels remained unchanged in ECs attached to FN (Fig. 3a). These data suggest that matrix-specific differences in PKA activity are likely mediated by differential cAMP production.

We next set out to investigate the mechanism of cAMP production on CL. cAMP production is often stimulated via $G\alpha_s$-associated G-protein coupled receptors (GPCRs) that promote production of the nucleotide via activation of adenylyl cyclase. In order to test if force-dependent PKA activation on CL was mediated by a GPCR, ECs were pretreated with a general G-protein inhibitor (GDP-β-S) prior to force application on PECAM-1. Cells treated with vehicle displayed a significant increase in pPKA levels, while inhibition of G-protein signaling abolished force-dependent PKA activation on CL (Fig. 3b). Similarly, G-protein inhibition also blocked force-induced CREB phosphorylation in ECs attached to CL

(Supplementary Fig. 3). To specifically test for involvement of $G\alpha_s$-dependent signaling, ECs were depleted of $G\alpha_s$ using specific siRNAs. ECs adherent to CL and lacking $G\alpha_s$ did not display mechanosensitive activation of PKA, while control cells demonstrated an increase in pPKA levels in response to force on PECAM-1 (Fig. 3c). Therefore, our data suggest that CL-specific mechanosensitive activation of $G\alpha_s$ signaling results in matrix-specific cAMP production and subsequent activation of PKA.

Mechanically-induced PKA activity negatively regulates RhoA

ECs attached to CL do not generate a mechanical response when tension is applied to PECAM-1 (Fig. 1) and show differential activation of the PKA and RhoA pathways, when compared to cells adherent on FN (Fig. 2). Given that PKA-dependent phosphorylation of RhoA has been shown to negatively regulate activity of the GTPase in other systems, we hypothesized that PKA phosphorylates RhoA and attenuates force-dependent RhoA activation in ECs adherent on CL. In order to test this hypothesis, levels of RhoA serine phosphorylation following force application on PECAM-1 were assessed by immunoprecipitation and immunoblot analysis (Fig. 4a). Indeed, ECs exhibited force-induced serine phosphorylation in response to tension on PECAM-1, suggesting that RhoA may be inactivated via serine phosphorylation at later time points. In order to test if PKA mediates force-induced serine phosphorylation of RhoA, ECs were pretreated with the PKA inhibitor PKI, prior to mechanical stimulation. Consistent with our hypothesis, PKA inhibition completely abolished force-dependent RhoA phosphorylation (Fig. 4b). These data indicate that force-induced activation of PKA promotes phosphorylation and inactivation of RhoA in ECs adherent on CL. Thus, we reasoned that abrogation of PKA signaling and therefore, inhibition of RhoA serine phosphorylation, should also influence levels of active or GTP-bound RhoA in response to tension on PECAM-1. In agreement with our hypothesis, blockade of PKA signaling resulted in robust and sustained activation of RhoA (Fig. 4c). Taken together, these data indicate that PKA activation modulates RhoA serine phosphorylation and, thus, activity of the GTPase in response to tension on PECAM-1.

PKA inhibition confers mechano-responsiveness to ECs on CL

In light of these data, we hypothesized that inhibition of PKA (and prolonged activation of RhoA) may confer the stiffening response to ECs adherent on CL. To address this, we pretreated ECs with the PKA inhibitor prior to stimulating PECAM-1 in the magnetic tweezers system. Control ECs did not respond to tension on PECAM-1 (similar to Fig. 1b). In contrast, inhibition of PKA signaling resulted in a rapid and significant adaptive stiffening response (Fig. 5a). In addition, knockdown of the catalytic subunit of PKA using specific siRNAs also induced a significant stiffening response in ECs plated on CL (Supplementary Fig. 4). These data suggest that prolonged activation of RhoA is sufficient to restore mechanical responsiveness to tension on PECAM-1. In order to examine if inhibition of PKA permitted force-induced growth of focal adhesions in cells attached to CL, ECs pretreated with PKI were subjected to force and immunostained for the focal adhesion protein vinculin. In agreement with our magnetic tweezers studies, blockade of PKA signaling resulted in a significant increase in focal adhesion size and number, whereas vehicle-treated ECs did not exhibit significant focal adhesion growth (Fig. 5b). Thus, our

data indicate that suppression of PKA signaling restores the mechanical response to tension on PECAM-1.

PKA inhibits haemodynamic-induced focal adhesion growth

Our data indicate that PKA is responsible for regulating matrix-dependent stiffening and focal adhesion growth in response to applied magnetic forces. However, the haemodynamic force of fluid shear stress is the critical physiological force *in vivo*. ECs subjected to shear stress remodel their focal adhesions in order to resist shear forces[21, 22], and PECAM-1 is part of a mechanosensory complex that influences cytoskeleton dynamics in ECs subjected to fluid shear stress[15]. Therefore, we extended our studies to investigate the role of the PKA pathway in EC focal adhesion dynamics in response fluid shear stress. ECs plated on CL were subjected to shear stress (12 dyn/cm^2) and immunostained for vinculin to highlight focal adhesions (Fig. 6a). ECs subjected to shear displayed a 2-fold increase in focal adhesion number (Supplementary Fig. 5a), consistent with previous reports[22]. Furthermore, we found that inhibition of PKA signaling significantly augmented shear-induced focal adhesion growth (Fig. 4a), similar to the growth of focal adhesions observed when tension was applied on PECAM-1 (Fig. 3b). It is important to note that inhibition of PKA did not significantly influence focal adhesion size or number in the absence of shear stress (Supplementary Fig. 5b). Next, we tested if PECAM-1 was required for PKA-mediated suppression of focal adhesion growth by subjecting PECAM-1$^{-/-}$ ECs to shear stress. Inhibition of PKA signaling did not affect focal adhesion growth in PECAM-1$^{-/-}$ ECs (PE-KO) in response to shear stress, whereas null cells engineered to re-express PECAM-1 (PE-RC) displayed a significant increase focal adhesion growth, similar to the effect seen in bovine aortic ECs (Supplementary Fig. 6, Fig. 6a). Thus, these data indicate that PECAM-1-dependent PKA signaling regulates focal adhesion dynamics in response to the physiological stimulus of fluid shear stress.

We sought to extend our *in vitro* shear stress studies to an *in vivo* setting. We examined focal adhesions in the descending aorta, as it is rich in CL composition and experiences relatively uniform shear stress patterns. In order to test if PKA regulates focal adhesion growth *in vivo*, wildtype mice were injected with PKA inhibitor (PKI) or vehicle (DMSO). Two hours after injection, the descending aorta was harvested and *en face* preparations were immunostained for vinculin to highlight focal adhesions in the endothelium. Remarkably, inhibition of PKA signaling *in vivo* resulted in a significant increase in the number of focal adhesions present in the descending aorta (Fig. 6b) compared to control, suggesting that the PKA pathway is also a critical regulator of focal adhesion dynamics in ECs in the haemodynamic environment of the vessel.

PKA promotes EC compliance in CL-rich regions of the aorta

Several studies have suggested a link between vessel stiffness and cardiovascular disease[9, 10, 11]. However, measurements of EC stiffness *ex vivo* are lacking and the mechanisms that govern aortic EC stiffness remain largely unexplored. Our *in vitro* data suggest that growth of focal adhesions corresponds with a stiffer EC phenotype and that activation of the PKA pathway exerts a negative effect on active stiffening responses via inhibition of RhoA signaling. In contrast, suppression of PKA signaling restores

mechanotransduction in response to tension on PECAM-1 (Fig. 5), shear stress application *in vitro* (Fig. 6a), and in the haemodynamic environment of the blood vessel (Fig. 6b). In order to test the direct physiological relevance of these effects, we used external passive microbead rheology[23] to determine whether the PKA pathway is also a determinant of EC stiffness *in vivo*. The descending aorta was freshly isolated from control or PKI-treated mice two hours after injection and prepared *en face* to expose the endothelium for passive microbead rheology measurements. The descending aorta was incubated with FN-conjugated beads in order to establish integrin-mediated attachments with the cortical actin cytoskeleton. Thermal motion of attached beads was tracked and the resulting mean-squared displacements (MSD) were calculated for control or PKI-treated aortas (Fig. 7a,b). Of note, MSD trajectories show a slope less than unity (illustrated by black guide line in Fig 7e), indicating a sub-diffusive viscoelastic response consistent with the movements of beads anchored to the actin cytoskeleton via integrins[24]. Ensemble-averaging of the bead populations revealed a significant decrease in MSD magnitude in PKI-treated descending aortas compared to control descending aortas (Fig. 7e). Furthermore, calculation of the average root mean-squared (RMS) at the 1-second timescale for each condition revealed a significant decrease in the effective radius of bead displacement in PKI-treated aortas (Fig. 7f). These data suggest a significant increase in stiffness in the endothelium of PKI-treated descending aortas compared to controls. Thus, the PKA pathway appears to be a significant regulator of EC stiffness in the CL-rich descending aorta.

The aorta is heterogeneous in matrix composition, such that healthy, atheroresistant regions of the aorta (such as the descending aorta) are rich in CL content, whereas atheroprone regions of the aorta (such as the aortic arch) that are susceptible to inflammation and disease have a relatively FN content (Fig. 7c). Our *in vitro* data suggest that, when tension is applied to PECAM-1, FN content promotes a stiffer EC phenotype, while stiffening is actively inhibited in ECs attached to CL. Therefore, we hypothesized that ECs located in atheroprone regions of the aorta would exhibit increased stiffness compared to EC situated in atheroresistant regions. Atheroprone aortic arches were harvested and external passive microbead rheology revealed a significant decrease in MSD magnitude in atheroprone regions of the aorta compared to atheroresistant regions (Fig. 7d,e). Furthermore, calculation of the RMS at the 1-second timescale revealed a significant decrease in the effective radius of bead displacement in atheroprone aortic arch compared to the atheroresistant descending aorta (Fig. 7f). These data suggest a significant increase in stiffness in the ECs located in the FN-rich aortic arch, compared to ECs that reside within the CL-rich descending aorta. Given that inflammation and formation of atherosclerotic plaques preferentially develop in atheroprone regions of the vessel, such as the aortic arch, our data are also consistent with the idea that EC stiffness may be correlated to vascular disease. It is also important to note that inhibition of PKA signaling in the descending aorta increased EC stiffness values towards those observed in atheroprone regions of the aortic arch (Fig. 7e,f). Thus, our data indicate that PKA actively suppresses EC stiffening in healthy regions of the vessel and may play a critical role in maintaining vessel integrity *in vivo*.

Discussion

Here we identify a novel pathway that regulates endothelial mechanical responses and determines aortic EC stiffness, which may contribute to maintenance of blood vessel integrity. We sought out to determine the role of ECM identity in PECAM-1-mediated mechanotransduction and discovered that while some responses are common, ECs adherent on CL display divergent signaling in response to mechanical tension on PECAM-1 compared to ECs adherent on FN. Although tension on PECAM-1 induces PI3K and downstream integrin activation, ECs on do not generate a stiffening response, which may be partially attributed to reduced focal adhesion remodeling. Mechanistically, we demonstrate that mechanical tension on PECAM-1 results in Gαs-mediated cAMP production, PKA activation and Ser188 phosphorylation of RhoA, which results in its deactivation. Inhibition of PKA signaling prolongs force-induced RhoA activation and results in cellular stiffening and focal adhesion growth in response to force (Fig. 8). We further extended these findings to the physiological haemodynamic stimulus of fluid shear stress and reveal that PKA negatively regulates focal adhesion dynamics in ECs *in vitro* and in the haemodynamic environment of the vessel *in vivo.* Our *in vivo* studies suggest that this is a physiologically relevant signaling cascade, as ECs located in regions of the aorta where CL is the dominant ECM protein are more compliant than ECs located in FN-rich regions of the vessel. Finally, we highlight PKA as a critical regulator of EC mechanics in collagen-rich regions of the aorta and demonstrate active regulation of aortic EC stiffness *in vivo*.

PKA is a multifunctional protein that has many roles in cell biology. Within the endothelium, the kinase has well documented roles in anti-inflammatory signaling[15], angiogenesis[25], barrier function[26, 27], and cell migration[28]. Importantly, PKA-mediated RhoA inactivation has been shown to regulate endothelial barrier function *in vitro*[26], and the kinase has been shown to tightly regulate RhoA activity during protrusion-retraction cycles in migrating cells[28, 29]. In this study, we systemically delivered a PKA inhibitor in order to examine effects on focal adhesion dynamics and EC compliance. Previous studies have demonstrated that inhibition of PKA signaling can promote inflammation and influence EC permeability[18,26]. It is possible that we could have affected these factors in our study, especially since EC stiffness and permeability are linked. However, our *in vitro* and *in vivo* studies clearly implicate PKA as a regulator of EC compliance. Future studies exploring the relationship between inflammation, EC compliance, and permeability may provide valuable insights into factors that influence vessel health.

Our *in vitro* studies also indicate that PKA inhibition of RhoA signaling influences EC responsiveness to force and focal adhesion dynamics. PKA can directly phosphorylate RhoA at serine 188, and phosphorylation of this residue inhibits activity of the GTPase[20, 29]. Serine phosphorylation of RhoA increases its association with Rho-GDI and negatively influences activity by sequestering the GTPase in the cytoplasm[30]. In addition to its role regulating RhoA activity, a complex relationship between PKA and integrin-mediated adhesion also exists. Detachment of cells from the ECM triggers robust, but transient, activation of the kinase[31, 32]. Conversely, integrin-mediated adhesion also stimulates PKA activation and is important for strengthening cell-cell and cell-matrix adhesions in certain cell types[33].

Our work highlights RhoA as a critical regulator of the cellular response to force. While mechanical stimulation of PECAM-1 induces RhoA activation in ECs adherent on CL, activation is transient and insufficient to initiate adaptive stiffening and focal adhesion growth. While we provide evidence for RhoA inactivation via serine phosphorylation, it is possible that force-dependent changes in GEF and GAP activity may also contribute to transient activation of the GTPase. For instance, p190RhoGAP is rapidly phosphorylated in ECs exposed to shear stress, and the GAP is required for flow-mediated changes in the actin cytoskeleton[34]. Therefore, it is possible that force-dependent activation of p190RhoGAP may also influence RhoA activity. In addition, previous work from our lab identified activation of the RhoGEF GEF-H1 in response to tension on PECAM-1[12]. Others have shown that PKA-dependent phosphorylation of GEF-H1 suppresses its GEF activity[35]. Therefore, it is also possible that force-dependent PKA activation inhibits GEF-H1-mediated GTP-loading at later time points. Nevertheless, our results clearly indicate that PKA regulates RhoA activity and the cellular response to mechanical force.

Increased vessel stiffness is often associated with various vascular pathologies, therefore understanding factors that contribute to EC stiffness *in vivo* is critical. Despite the association of vascular stiffness with disease, measurements of EC stiffness *in vivo* are lacking and mechanisms that regulate EC stiffness remain largely unexplored. Here, we report that EC stiffness *in vivo* is heterogeneous and site-specific, such that ECs in FN-rich regions of the aorta prone to atherosclerosis are stiffer than those in atheroresistant regions. Furthermore, we identify PKA as an active regulator of EC compliance in atheroresistant regions of the aorta, as PKA inhibition promotes focal adhesion growth and increases EC stiffness in the descending aorta. The descending aorta is rich in CL composition and, notably, more resistant to atherosclerotic plaque development compared to other regions of the vasculature. Additionally, vessel stiffness positively correlates with EC permeability and leukocyte transmigration[11], and thus, contributes to the development of vascular disease. Therefore, PKA-mediated suppression of RhoA activity, inhibition of focal adhesion growth and increased EC compliance in the descending aorta may serve as a protective mechanism that maintains endothelial barrier function and regulates permeability.

Overall, our work identifies a unique mechanosensitive and ECM-dependent signaling pathway that regulates EC stiffness and focal adhesion dynamics. Using magnetic tweezers, we show that tension on PECAM-1 initiates an intracellular signaling cascade that regulates the cellular force response and focal adhesion growth. We report that EC stiffness differs in regions of the aorta where different ECM compositions have been reported, and demonstrate that ECs in regions of the vessel that contain a high FN content are stiffer than those in CL-rich regions of the aorta. Furthermore, we identify PECAM-1-dependent PKA signaling as a critical regulator of focal adhesion dynamics and EC stiffness *in vitro* and *in vivo*, which may function as an atheroprotective mechanism in distinct regions of the vasculature.

Methods

Cell culture and shear stress

Bovine aortic endothelial cells (a kind gift from Dr. Shu Chien's lab at UCSD) were maintained in Dulbecco's modified Eagle's medium (DMEM, Cellgro) with 10% fetal

bovine serum and 1% penicillin/streptomycin solution. PECAM-1 knockout (PE-KO) and reconstituted (PE-RC) cells were cultured in DMEM containing 10% FBS, 10 μM 2-mercaptoethanol (Invitrogen), 1× nonessential amino acids (NEAA; Invitrogen), and penicillin/streptomycin. Cells were plated on fibronectin (10 μg/ml) or Type I collagen (40 μg/ml) 4 hours prior to experiments. For shear stress experiments, endothelial cells were plated on 40 μg/ml collagen in 0.5% FBS. Four hours after plating, cells were slides were loaded onto a parallel plate flow chamber in 0.5% FBS and 12 dynes/cm^2 of shear stress was applied for indicated times, as previously described[36]. A surface area of 14 cm^2 on the BAEC-seeded slide was exposed to fluid shear stress generated by perfusing culture medium over the cells. The pH of the system was kept constant by gassing with 5% CO_2/95% air and the temperature was maintained at 37°C.

Inhibitors and antibodies

PKI was purchased from Calbiochem and was used at 20μM for 1hr to inhibit PKA activity. The PECAM-1 antibody used for bead coating (PECAM 1.3, 5μg/25μl beads) was a generous gift from D.K. Newman (BloodCenter of Wisconsin). The RhoA antibody (26C4) used for western blotting (1:300) were purchased from Santa Cruz Biotechnologies. The phospho-CREB (Ser133), phospho-PKA (Tyr-197) and total PKA antibodies were from Cell Signaling and were used at 1:1000 dilution for western blotting, and the phospho-serine antibody (1:1000 dilution for western blot) and rhodamine-phalloidin (1:100 dilution for immunofluorescence) were from Invitrogen. The actin (1:2000 dilution for immunoblot), vinculin (1:100 for immunofluorescence) and β-catenin (1:100 for immunofluorescence) antibodies and GDP-β-S (20μM, 30min) were obtained from Sigma, and the HUTS-4 antibody (which recognizes ligated β1 integrin) was purchased from Millipore and used at 1:100 dilution for immunofluorescence. The VE-cadherin antibody was from B.D. Pharminogen and was used at 1:100 dilution.

RNAi interference and transfections

For RNA interference experiments, control (Dharmacon siGLO RISC-free control siRNA), $G\alpha_s$, or PKA Cα siRNAs (Dharmacon) were transfected into cells using a calcium phosphate method. Briefly, 2.5M $CaCl_2$ was added to siRNA (5μM) diluted in 2X HBS. The transfection mixture was mixed vigorously, incubated for 20 min at room temperature and added dropwise to plate containing 50% confluent cells. Cells were plated on CL 96 hrs post-transfection and experiments were performed. The following siRNA sequences were used in this study: $G\alpha_s$: 5′-CCACCAAAGUGCAGGACAUUU-3′; PKA Cα: 5′-GAGUAAAGGCUACAACAAAUU -3′. For GFP-PH experiments, cells were seeded at 50% confluence and transfected with 2.5 μg of the GFP-PH construct using Effectene reagents (QIAGEN) according to the manufacturer's protocol. Experiments were performed 48 hr after transfection.

Preparation of beads

Tosyl-activated paramagnetic beads (2.8 or 4.5μm, Invitrogen) were washed with PBS and coated with an anti-PECAM-1 antibody (PECAM 1.3) or purified human fibronectin according to the manufacturer's protocol. Beads were quenched in 0.2M Tris prior to use to remove any remaining tosyl groups and were resuspended in PBS or DMEM containing

10% fetal bovine serum and 1% penicillin/streptomycin solution. Immediately before experiments, ECs were incubated with beads (2–6 bead/cell) for 30min at 37°C. Cells were briefly washed with fresh media to remove unbound beads prior to force application.

Pulsatile force application

The UNC 3D Force Microscope (3DFM) was used to apply controlled pulsatile forces (~100pN) to anti-PECAM-1-coated magnetic beads (2.8μm diameter). Bead displacements were recorded with a high-speed video camera (Pulnix, JAI) and tracked using Video Spot Tracker (Computer Integrated Systems for Microscopy and Manipulation, http://cismm.cs.unc.edu/).

Permanent force application

For all immunostaining and biochemical analyses, continuous force (~10pN) was applied to anti-PECAM-1-coated beads (4.5μm diameter) using a permanent ceramic magnet (K&J Magnetics) parallel to the cell culture dish at a distance of 1cm from the adherent cells.

Immunofluorescence

ECs grown on CL-coated cover slips and subjected to force (permanent magnet, 4.5μm beads) were fixed for 20 min in PBS containing 2% formaldehyde, permeabilized with 0.2% Triton X-100, and blocked with PBS containing 10% goat serum for 1hr at room temperature. Antibody incubations were performed as previously described[12]. Briefly, cells were incubated with specific primary antibodies (1:100) overnight at 4°C, briefly washed with PBS containing 0.001% Triton X-100, and then were incubated with a fluorescent secondary antibody for 1hr at room temperature. All cover slips were mounted in Vectashield mounting medium. Images were acquired using a confocal microscope (Olympus FV500) with a 63x oil lens.

cAMP measurements

To assay cAMP, cells were lysed in 0.1 N HCl supplemented with 0.1% Triton X-100 for 10min. Levels of cAMP were determined by competitive immunoassay (Sigma #CA200) according to the manufacturer's instructions. Samples were acetylated in order to increase assay sensitivity, and values were normalized to total protein levels.

Rho Pulldowns

Adherent cells grown on ECM-coated 10cm dishes were incubated with anti-PECAM-1-coated beads (4.5μm, Invitrogen) for 30 min and subjected to force for indicated times. Briefly, following force application, cells were lysed in 50mM Tris (pH 7.6), 500mM NaCl, 1% Triton X-100, 0.1% SDS, 0.5% deoxycholate, 10mM $MgCl_2$, and protease inhibitors. Anti-PECAM-1-coated magnetic beads were removed from lysates with a magnetic separator. Lysates were centrifuged for 5min and supernatants were transferred to a new tube and incubated at 4° with 80μg of purified (GST-RBD) bound to glutathione-sepharose beads. Bead pellets were washed in 50mM Tris (pH 7.6), 150mM NaCl, 1% Triton X-100, 10mM $MgCl_2$, and protease inhibitors, and subsequently resuspended in Laemmli sample buffer and subjected to SDS-PAGE.

Immunoprecipitation and western blotting

Cells grown in 10 cm dishes and subjected to force as described above were harvested in lysis buffer (20mM Tris (pH 7.4), 150mM NaCl, 50mM NaF, 1% NP-40) supplemented with 10 μg/ml aprotinin, 10 μg/ml leupeptin, 1 mM PMSF, 1 mM Na_3VO_4, 1 mM sodium pyrophosphate, and 1 mM β-glycerophosphate. Lysates were pre-cleared with 15μl protein A/G plus sepharose beads (Santa Cruz) for 1 h at 4°C. Supernatants were then incubated with 30μl protein A/G plus sepharose previously coupled to the primary antibodies for 3 h at 4°C with continuous agitation. The beads were washed three times with lysis buffer supplemented with protease and phosphatase inhibitors and the immune complexes were eluted in 2X SDS sample buffer. Associated proteins were subjected to SDS-PAGE and Western blotting using the appropriate primary antibodies and IRDye-conjugated anti-mouse or anti-rabbit antibodies (Rockland). Images of Western blotting were obtained with an Odyssey infrared scanner system.

Quantification of integrin activation and focal adhesions

ECs stained for ligated β1 integrin (Supplementary Fig. 2B) or vinculin were analyzed with NIH ImageJ software. Confocal image planes at the basal surface of the cell were chosen for analysis and RGB images were converted to 8-bit black and white images. Activated integrins and focal adhesions were defined by setting an intensity threshold to remove background signal. Integrin activation and focal adhesion size and number were analyzed using the 'Analyze particles' function.

Animals and *en face* aorta preparations

All mice were used in accordance with the guidelines of the National Institutes of Health and the care and use of laboratory animals (approved by the Institutional Animal Care and Use Committees of the University of North Carolina at Chapel Hill). 5nmol of PKI or DMSO was administered by retro-orbital injection into 10–14 wk old male C57BL/6 mice. Two hrs after injection, descending aortas were isolated and processed for *en face* immunostaining. Briefly, the aorta was perfusion-fixed and dissected out under dissection microscope. The descending aortas were cut longitudinally and pinned flat with endothelium facing up onto a Surperfrost/Plus glass slide (Fisher Scientific). Tissue sections were stained with anti-vinculin and anti-VE-cadherin antibodies an imaged as described above.

Passive microbead assay for analysis of aortic ECs

The aorta was freshly isolated and prepared *en face* on a cover slip. Briefly, the heart was perfused with PBS containing heparin and sodium nitroprusside and the live aorta was dissected out under a dissection microscope, cut longitudinally, and mounted on a glass coverslip with the endothelium facing up. To anchor the aorta to the cover slip for experiments, a thin sheet (approximately 20 x 40 x 2 mm) of polydimethylsiloxane rubber (PDMS) (Sylgard 184, Dow Corning) was positioned over the tissue. A small section (3 x 5 mm) of the PDMS sheet was removed previous to anchorage to serve as a media reservoir region of interest. The reservoir was immediately filled with Medium 199 containing 10% FBS and 15mM HEPES in order to keep the tissue alive. Fibronectin-conjugated paramagnetic beads (4.5μm, Invitrogen) were incubated over the endothelium for 20 minutes

at 37°C. The thermal motion of attached beads was imaged at 40X using an upright reflective microscope (Orthoplan, Leitz) and recorded at 30 frames per second with a high-speed video camera (Pulnix, JAI). Bead motion was monitored for 1 minute and tracked using Video Spot Tracker software (Computer Integrated Systems for Microscopy and Manipulation, http://cismm.cs.unc.edu/). The time-dependent mean-squared displacement (MSD) of the bead trajectories was computed using $<r^2(\tau)> = <\text{MSD}> = <[x(t+\tau)-x(t)]^2 + [y(t+\tau)-y(t)]^2>$, where t is the elapsed time and τ is the time lag, or timescale. Beads included into analysis were separated from other beads by 3 bead-diameters. Conditions were compared using the ensemble-averaged MSD and the root mean-squared (RMS) displacement.

Statistical analysis

Data are presented as means +/− S.E.M. p-values were determined using a two-tailed unpaired Student's *t*-test.

Supplementary Material

Refer to Web version on PubMed Central for supplementary material.

Acknowledgments

We would like to thank Dr. Robert Bagnell and the UNC Lineberger Cancer Center Microscopy Facility for help with microscopy studies. C.C. is an American Heart Association Predoctoral Fellow (12PRE119300000). C.G. is supported by a Marie Curie Outgoing International Fellowship from the European Union Seventh Framework Programme (FP7/2007–2013) under grant agreement number 254747. E.T. is an Ellison Medical Foundation New Scholar. This work was supported by NIH grants HL088632 (to E.T.), GM029860 (to K.B.), and 5P41EB002025 (to R.S.).

References

1. Wu CC, et al. Directional shear flow and Rho activation prevent the endothelial cell apoptosis induced by micropatterned anisotropic geometry. Proc Natl Acad Sci U S A. 2007; 104:1254–1259. [PubMed: 17229844]
2. Ohura N, et al. Global analysis of shear stress-responsive genes in vascular endothelial cells. J Atheroscler Thromb. 2003; 10:304–313. [PubMed: 14718748]
3. Mammoto A, et al. A mechanosensitive transcriptional mechanism that controls angiogenesis. Nature. 2009; 457:1103–1108. [PubMed: 19242469]
4. Chicurel ME, Singer RH, Meyer CJ, Ingber DE. Integrin binding and mechanical tension induce movement of mRNA and ribosomes to focal adhesions. Nature. 1998; 392:730–733. [PubMed: 9565036]
5. Weber GF, Bjerke MA, DeSimone DW. A mechanoresponsive cadherin-keratin complex directs polarized protrusive behavior and collective cell migration. Dev Cell. 2012; 22:104–115. [PubMed: 22169071]
6. Matthews BD, Overby DR, Mannix R, Ingber DE. Cellular adaptation to mechanical stress: role of integrins, Rho, cytoskeletal tension and mechanosensitive ion channels. J Cell Sci. 2006; 119:508–518. [PubMed: 16443749]
7. Guilluy C, Swaminathan V, Garcia-Mata R, O'Brien ET, Superfine R, Burridge K. The Rho GEFs LARG and GEF-H1 regulate the mechanical response to force on integrins. Nat Cell Biol. 2011; 13:722–727. [PubMed: 21572419]
8. Kuo JC, Han X, Hsiao CT, Yates JR 3rd, Waterman CM. Analysis of the myosin-II-responsive focal adhesion proteome reveals a role for beta-Pix in negative regulation of focal adhesion maturation. Nat Cell Biol. 2011; 13:383–393. [PubMed: 21423176]

9. Hirai T, Sasayama S, Kawasaki T, Yagi S. Stiffness of systemic arteries in patients with myocardial infarction. A noninvasive method to predict severity of coronary atherosclerosis. Circulation. 1989; 80:78–86. [PubMed: 2610739]
10. Wang YX, et al. Increased aortic stiffness assessed by pulse wave velocity in apolipoprotein E-deficient mice. Am J Physiol Heart Circ Physiol. 2000; 278:H428–434. [PubMed: 10666072]
11. Huynh J, et al. Age-related intimal stiffening enhances endothelial permeability and leukocyte transmigration. Sci Transl Med. 2011; 3:112ra122.
12. Collins C, et al. Localized tensional forces on PECAM-1 elicit a global mechanotransduction response via the integrin-RhoA pathway. Curr Biol. 2012; 22:2087–2094. [PubMed: 23084990]
13. Huveneers S, et al. Vinculin associates with endothelial VE-cadherin junctions to control force-dependent remodeling. J Cell Biol. 2012; 196:641–652. [PubMed: 22391038]
14. le Duc Q, et al. Vinculin potentiates E-cadherin mechanosensing and is recruited to actin-anchored sites within adherens junctions in a myosin II-dependent manner. J Cell Biol. 2010; 189:1107–1115. [PubMed: 20584916]
15. Tzima E, et al. A mechanosensory complex that mediates the endothelial cell response to fluid shear stress. Nature. 2005; 437:426–431. [PubMed: 16163360]
16. Orr AW, Ginsberg MH, Shattil SJ, Deckmyn H, Schwartz MA. Matrix-specific suppression of integrin activation in shear stress signaling. Mol Biol Cell. 2006; 17:4686–4697. [PubMed: 16928957]
17. Jalali S, et al. Integrin-mediated mechanotransduction requires its dynamic interaction with specific extracellular matrix (ECM) ligands. Proc Natl Acad Sci U S A. 2001; 98:1042–1046. [PubMed: 11158591]
18. Funk SD, Yurdagul A Jr, Green JM, Jhaveri KA, Schwartz MA, Orr AW. Matrix-specific protein kinase A signaling regulates p21-activated kinase activation by flow in endothelial cells. Circ Res. 2010; 106:1394–1403. [PubMed: 20224042]
19. Riveline D, et al. Focal contacts as mechanosensors: externally applied local mechanical force induces growth of focal contacts by an mDia1-dependent and ROCK-independent mechanism. J Cell Biol. 2001; 153:1175–1186. [PubMed: 11402062]
20. Ellerbroek SM, Wennerberg K, Burridge K. Serine phosphorylation negatively regulates RhoA in vivo. J Biol Chem. 2003; 278:19023–19031. [PubMed: 12654918]
21. Mott RE, Helmke BP. Mapping the dynamics of shear stress-induced structural changes in endothelial cells. Am J Physiol Cell Physiol. 2007; 293:C1616–1626. [PubMed: 17855768]
22. Davies PF, Robotewskyj A, Griem ML. Quantitative studies of endothelial cell adhesion. Directional remodeling of focal adhesion sites in response to flow forces. J Clin Invest. 1994; 93:2031–2038. [PubMed: 8182135]
23. Hoffman BD, Massiera G, Van Citters KM, Crocker JC. The consensus mechanics of cultured mammalian cells. Proc Natl Acad Sci U S A. 2006; 103:10259–10264. [PubMed: 16793927]
24. Wirtz D. Particle-tracking microrheology of living cells: principles and applications. Annu Rev Biophys. 2009; 38:301–326. [PubMed: 19416071]
25. Jin H, Garmy-Susini B, Avraamides CJ, Stoletov K, Klemke RL, Varner JA. A PKA-Csk-pp60Src signaling pathway regulates the switch between endothelial cell invasion and cell-cell adhesion during vascular sprouting. Blood. 2010; 116:5773–5783. [PubMed: 20826718]
26. Qiao J, Huang F, Lum H. PKA inhibits RhoA activation: a protection mechanism against endothelial barrier dysfunction. Am J Physiol Lung Cell Mol Physiol. 2003; 284:L972–980. [PubMed: 12588708]
27. Birukova AA, Burdette D, Moldobaeva N, Xing J, Fu P, Birukov KG. Rac GTPase is a hub for protein kinase A and Epac signaling in endothelial barrier protection by cAMP. Microvasc Res. 2010; 79:128–138. [PubMed: 19962392]
28. Tkachenko E, et al. Protein kinase A governs a RhoA-RhoGDI protrusion-retraction pacemaker in migrating cells. Nat Cell Biol. 2011; 13:660–667. [PubMed: 21572420]
29. Lang P, Gesbert F, Delespine-Carmagnat M, Stancou R, Pouchelet M, Bertoglio J. Protein kinase A phosphorylation of RhoA mediates the morphological and functional effects of cyclic AMP in cytotoxic lymphocytes. EMBO J. 1996; 15:510–519. [PubMed: 8599934]

30. Forget MA, Desrosiers RR, Gingras D, Beliveau R. Phosphorylation states of Cdc42 and RhoA regulate their interactions with Rho GDP dissociation inhibitor and their extraction from biological membranes. Biochem J. 2002; 361:243–254. [PubMed: 11772396]

31. Howe AK, Juliano RL. Regulation of anchorage-dependent signal transduction by protein kinase A and p21-activated kinase. Nat Cell Biol. 2000; 2:593–600. [PubMed: 10980699]

32. Howe AK, Hogan BP, Juliano RL. Regulation of vasodilator-stimulated phosphoprotein phosphorylation and interaction with Abl by protein kinase A and cell adhesion. J Biol Chem. 2002; 277:38121–38126. [PubMed: 12087107]

33. Whittard JD, Akiyama SK. Positive regulation of cell-cell and cell-substrate adhesion by protein kinase A. J Cell Sci. 2001; 114:3265–3272. [PubMed: 11591815]

34. Yang B, Radel C, Hughes D, Kelemen S, Rizzo V. p190 RhoGTPase-activating protein links the beta1 integrin/caveolin-1 mechanosignaling complex to RhoA and actin remodeling. Arterioscler Thromb Vasc Biol. 2011; 31:376–383. [PubMed: 21051664]

35. Meiri D, et al. Modulation of Rho guanine exchange factor Lfc activity by protein kinase A-mediated phosphorylation. Mol Cell Biol. 2009; 29:5963–5973. [PubMed: 19667072]

36. Tzima E, del Pozo MA, Shattil SJ, Chien S, Schwartz MA. Activation of integrins in endothelial cells by fluid shear stress mediates Rho-dependent cytoskeletal alignment. EMBO J. 2001; 20:4639–4647. [PubMed: 11532928]

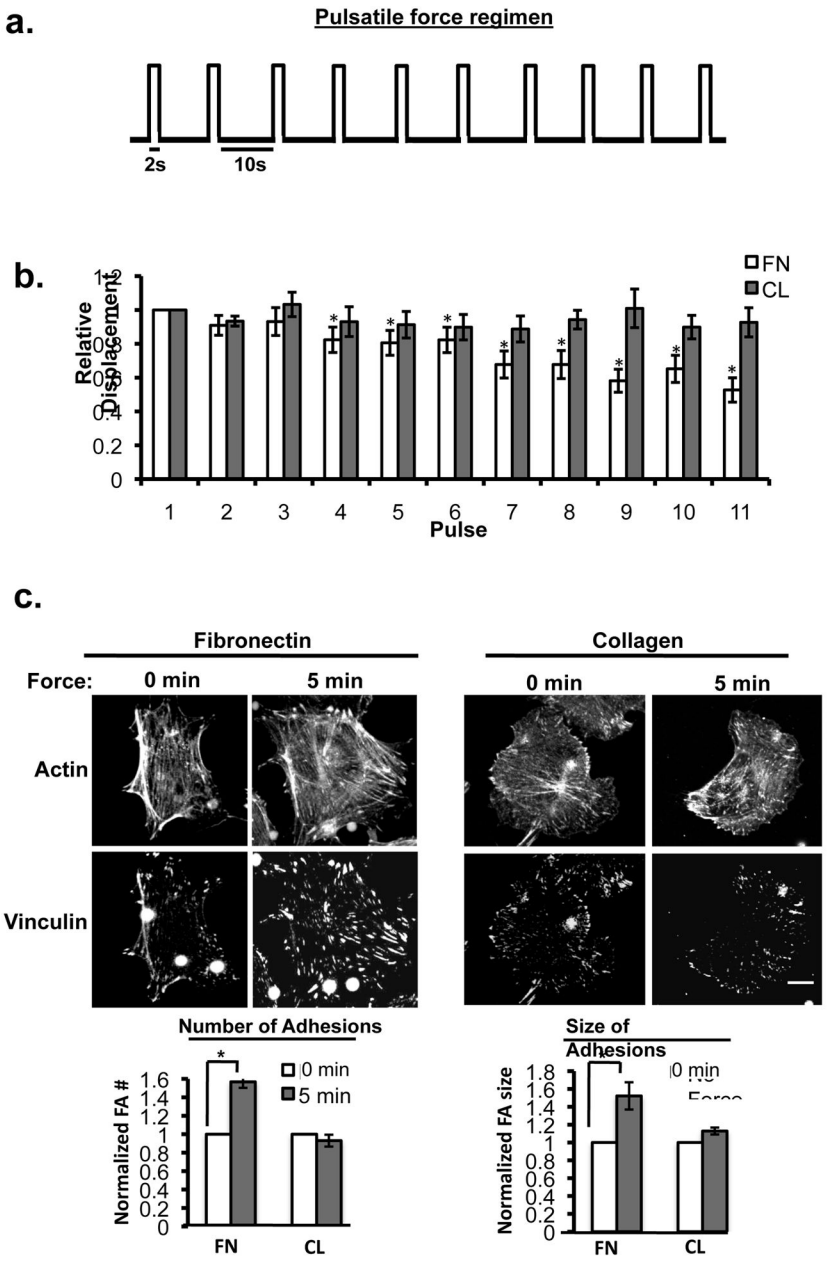

Figure 1. ECM composition determines the cellular response to tension on PECAM-1

(a) Pulsatile force regimen applied with magnetic tweezers, consisting of a 2 second, 100-pN pulse of force, followed by a 10 second period of rest, repeated over a 2 minute time course. (b) Average relative anti-PECAM-1-coated bead displacements induced by pulsatile force regimen. ECs were seeded on FN or CL 4 hrs prior to incubation with magnetic beads. Average displacements were calculated relative to the first pulse of force. (n >30 beads/condition from 3 independent experiments). Error bars represent s.e.m., *p<0.05 using a Student's *t*-test. (c) Adherent ECs on FN or CL were incubated with anti-PECAM-1-coated magnetic beads and subjected to force with a permanent magnet for the indicated times. ECs were fixed stained with phalloidin and an anti-vinculin antibody to mark focal adhesions.

Focal adhesion number and size were quantified using NIH ImageJ software. Values were normalized to the FN “No Force” condition. n > 30cells/condition from 3 independent experiments, *p < 0.05 using a Student’s *t*-test, scale bar = 10μm.

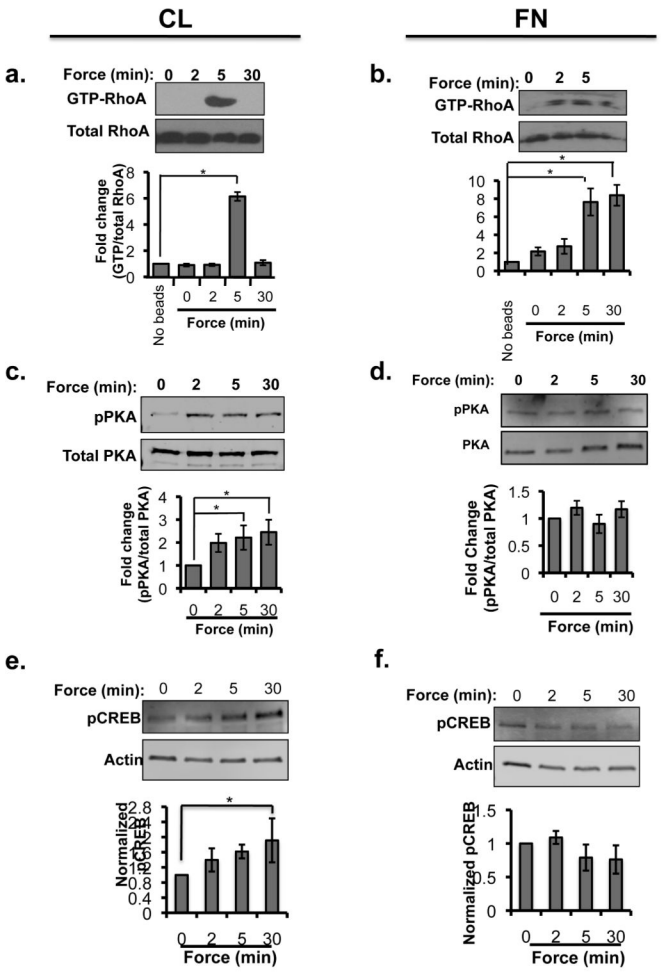

Figure 2. ECM composition regulates mechanosensitive activation of the PKA-RhoA pathway

(a–f) Tension was applied to anti-PECAM-1-coated beads using a permanent ceramic magnet for the indicated times, and (a) Active RhoA (RhoA-GTP) was isolated from EC adherent on CL with GST-RBD and analyzed by western blot (n=5). (b) Active RhoA (RhoA-GTP) was isolated from EC adherent on FN with GST-RBD and analyzed by western blot (n=5). (c) Cell lysates from ECs attached to CL were subjected to SDS-PAGE and immunoblotted for phospho (Tyr197) and total PKA (n=3). (d) Cell lysates from ECs adherent to FN were subjected to SDS-PAGE and immunoblotted for phospho (Tyr197) and total PKA (n=3). (e) Cell lysates from ECs adhered to CL were subjected to SDS-PAGE and immunoblotted for phospho-CREB (Ser133) and actin (n=3). (f) Cell lysates from ECs adherent on FN were subjected to SDS-PAGE and immunoblotted for phospho-CREB (Ser133) and actin (n=3). Bar graphs display averages from at least three independent experiments and error bars indicate s.e.m, *p<0.05 using a Student's *t*-test.

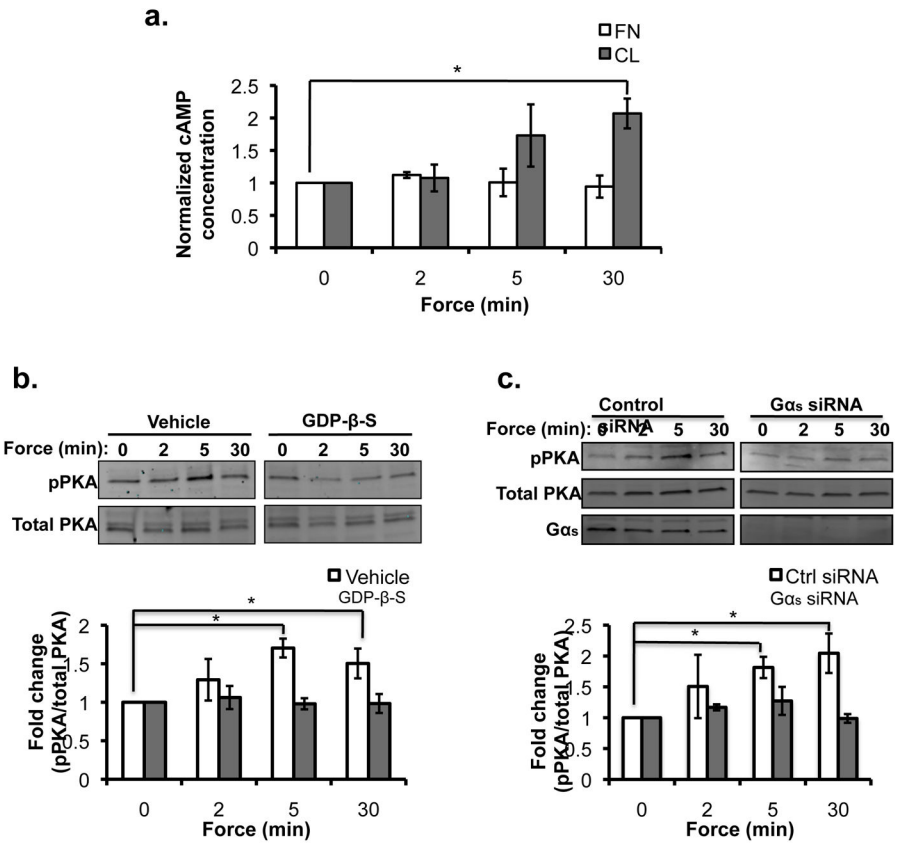

Figure 3. CL-specific mechanosensitive PKA activation is mediated by $G\alpha_s$-dependent cAMP production

(a-e) Tension was applied to anti-PECAM-1-coated beads using a permanent ceramic magnet for the indicated times, and (a) cAMP levels were measured by non-radioactive, competitive immunoassay (n=3). (b) ECs adherent on CL were pretreated with vehicle or GDP-β-S (20μM, 30min), subjected to force, and processed for SDS-PAGE. Lysates were immunoblotted for phospho (Tyr197) PKA and total PKA (n=3). (c) ECs adherent on CL were transfected with control or $G\alpha_s$-specific siRNAs. 96hrs after transfection, ECs were subjected to force and processed for SDS-PAGE. Lysates were immunoblotted for phospho (Tyr197) PKA and total PKA (n=3). Bar graphs display averages from at least three independent experiments and error bars indicate s.e.m, *p<0.05 (Student's *t*-test).

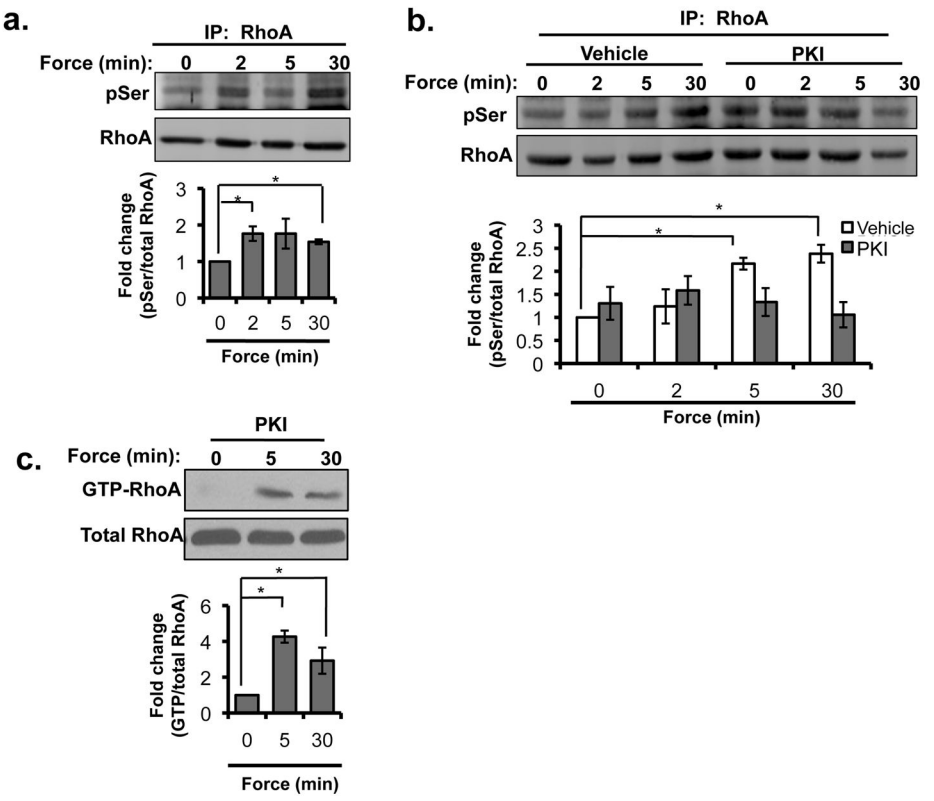

Figure 4. Mechanically-induced PKA activity negatively regulates RhoA

(a-c) Tension was applied to anti-PECAM-1-coated beads using a permanent ceramic magnet for the indicated times, and (a) Total RhoA protein was immunoprecipitated from cell lysates and immune complexes were subjected to SDS-PAGE, followed by immunoblotting with phosphoserine and RhoA antibodies (n=3). (b-c) ECs were treated with PKI (20μM for 1hr) or DMSO and tension was applied to anti-PECAM-1-coated beads using a permanent ceramic magnet for the indicated times. (b) Total RhoA protein was immunoprecipitated from cell lysates and immune complexes were subjected to SDS-PAGE, followed by immunoblotting with phosphoserine and RhoA antibodies (n=3). (c) Active RhoA (RhoA-GTP) was isolated with GST-RBD and analyzed by western blot (n=3). Bar graphs display averages from at least three independent experiments and error bars indicate s.e.m, *p<0.05 using a Student's *t*-test.

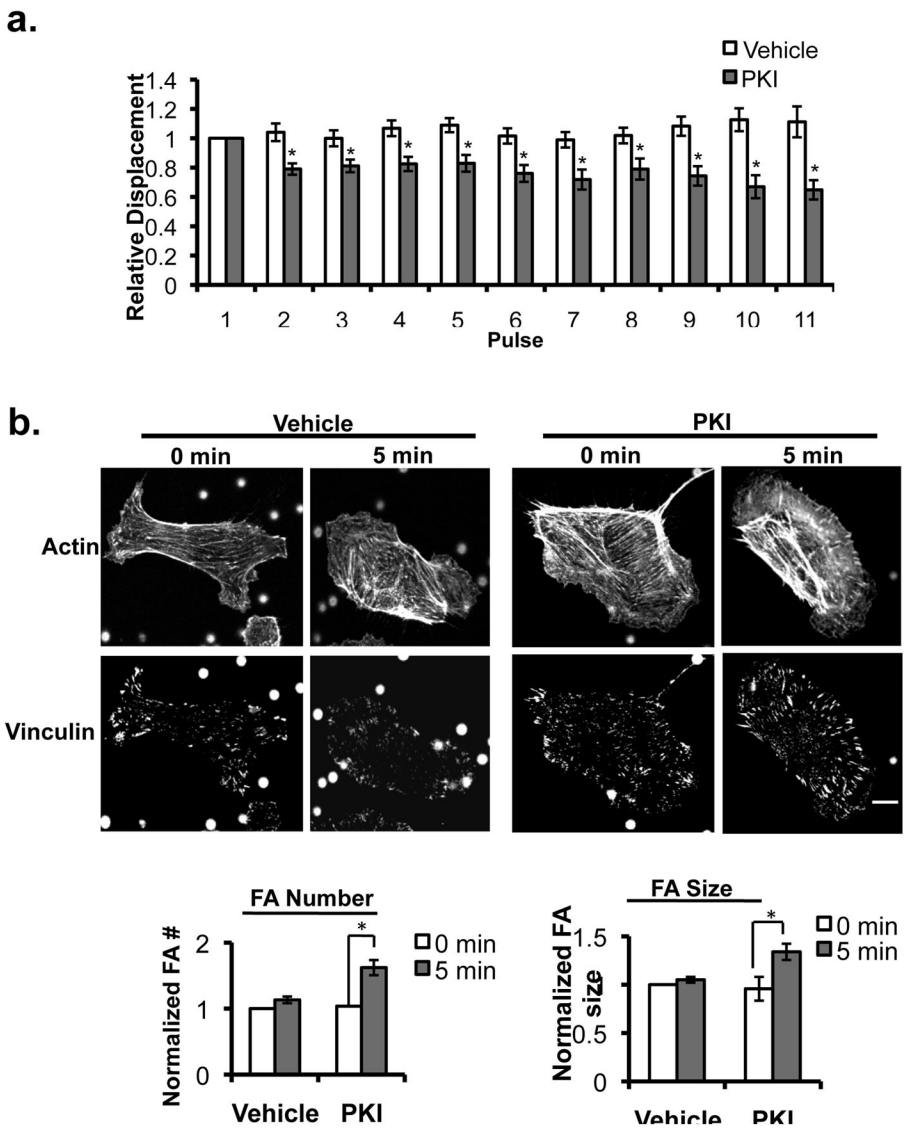

Figure 5. Inhibition of PKA confers mechanical responsiveness to ECs on CL

(a–b) ECs were pretreated with PKI (20μM) or vehicle for 1 hr, and (a) Pulsatile forces were applied to PECAM-1 with magnetic tweezers. Average relative anti-PECAM-1-coated bead displacements induced by pulsatile force regimen. Average displacements were calculated relative to the first pulse of force. (n >20 beads/condition from 3 independent experiments). (b) Anti-PECAM-1-coated magnetic beads were subjected to force with a permanent ceramic magnet for the indicated times. ECs were fixed stained with phalloidin and an anti-vinculin antibody to mark focal adhesions. Focal adhesion number and size were quantified using NIH ImageJ software. Values were normalized to the DMSO “No Force” condition. n > 30cells/condition from 3 independent experiments, *p < 0.05 using Student’s *t*-test, scale bar = 10μm.

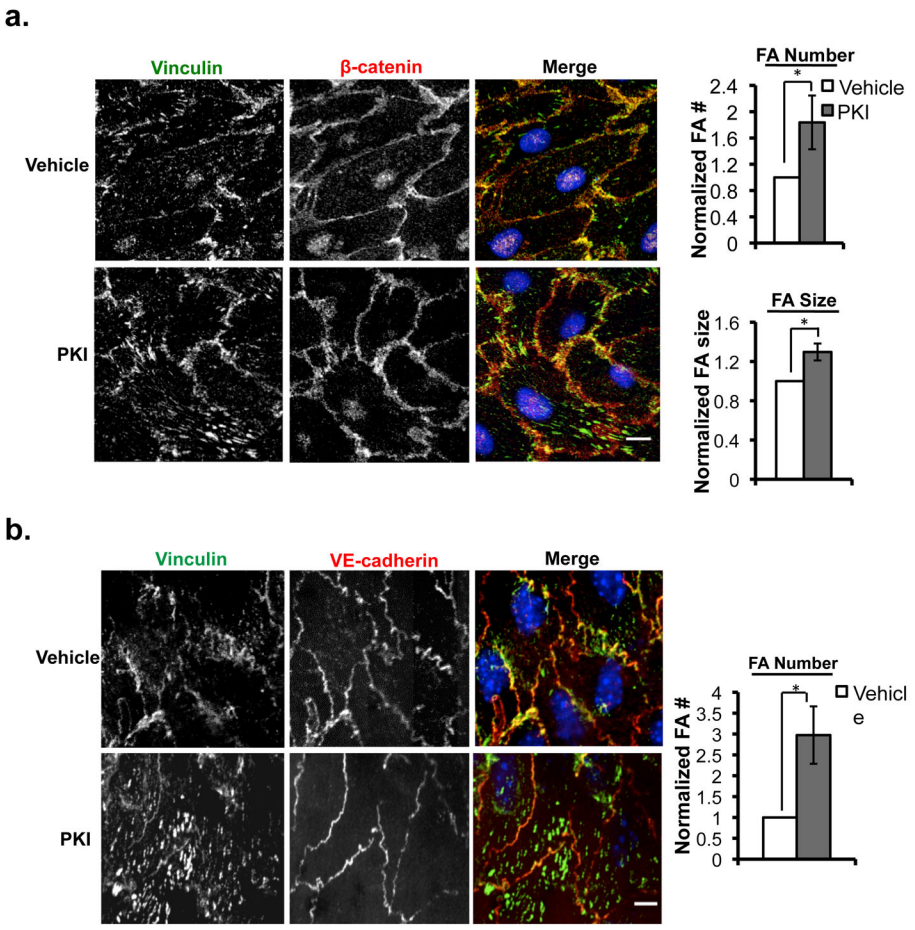

Figure 6. The PKA pathway regulates haemodynamic-induced focal adhesion dynamics *in vitro* and *in vivo*

(a) ECs adherent on CL pretreated with PKI (20μM, 1 hr) or vehicle and subjected to shear stress (12 dyn/cm^2 for 30min). Cells were fixed and immunostained with anti-vinculin and anti-β-catenin antibodies. Focal adhesion number and size were quantified using NIH ImageJ software. Values were normalized to the vehicle condition (n=3), *$p < 0.05$ using a Student's *t*-test, scale bar = 10μm. (b) Vehicle or PKI (5nmol) was administered to wildtype mice by retro-orbital injection. Two hrs after injection, aortas were harvested and *en face* preparations were immunostained with anti-vinculin and anti-VE-cadherin antibodies. Focal adhesions were quantified using NIH ImageJ software. Values were normalized to the vehicle (condition for each genotype (n=4 mice/group), *$p < 0.05$ using a Student's *t*-test, scale bar = 10μm.

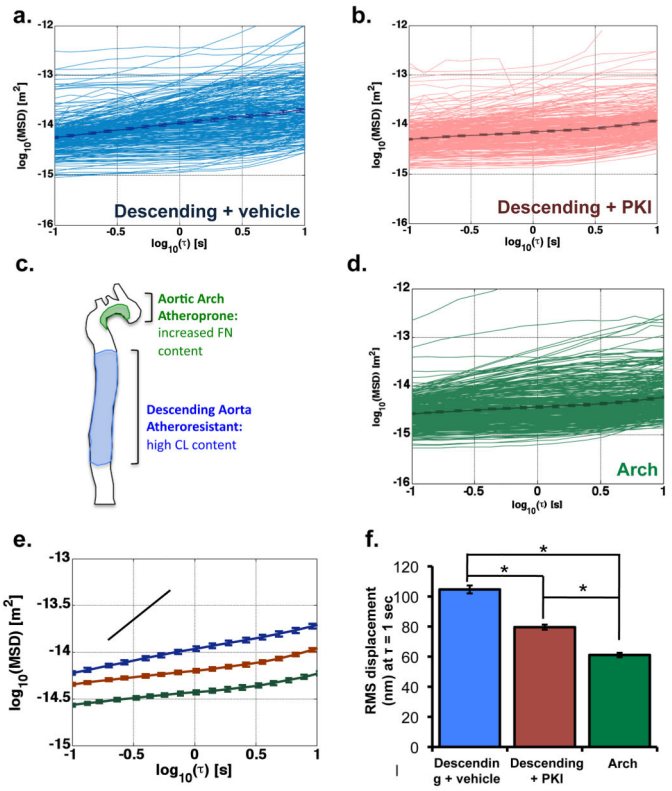

Figure 7. The PKA pathway promotes EC compliance in atheroresistant regions of the aorta

(a) Mean-squared displacement (MSD) trajectories of FN-conjugated, 4.5 μm beads attached to the atheroresistant region of the aorta. MSDs of individual curves (n > 350 per condition, aggregated from three mice) are shown in light color and the ensemble-average is represented by the dark curve with s.e.m. shown for indicated timescales. (b) MSD trajectories of FN-conjugated, 4.5 μm beads attached to the descending aorta from PKI-treated mice. MSDs of individual curves (n > 350 per condition, aggregated from three mice) are shown in light color and the ensemble-average is represented by the dark curve with s.e.m. shown for indicated timescales. (c) Diagram depicting ECM heterogeneity in the aorta. Regions of the aorta with high FN content are more prone to inflammation and disease, whereas regions with relatively high CL content are resistant to disease. (d) MSD trajectories of FN-conjugated, 4.5 μm beads attached to the atherprone (aortic arch) regions of the aorta. MSDs of individual curves (n > 350 per condition, aggregated from three mice) are shown in light color and the ensemble-average is represented by the dark curve with s.e.m. shown for indicated timescales. (e) Ensemble-averaged MSDs of beads attached to endothelium of aortic preparations. Curves show a slope less than unity (illustrated by black guide line), indicating a sub-diffusive viscoelastic response of beads anchored to the cortical actin cytoskeleton through apical integrin receptors. (f) Root mean-squared (RMS) displacement at the 1-second timescale ($\tau = 1$ s) of beads attached to endothelium in the descending aorta (+ vehicle or PKI) and the aorta arch, *p < 0.0001 using a Student's *t*-test.

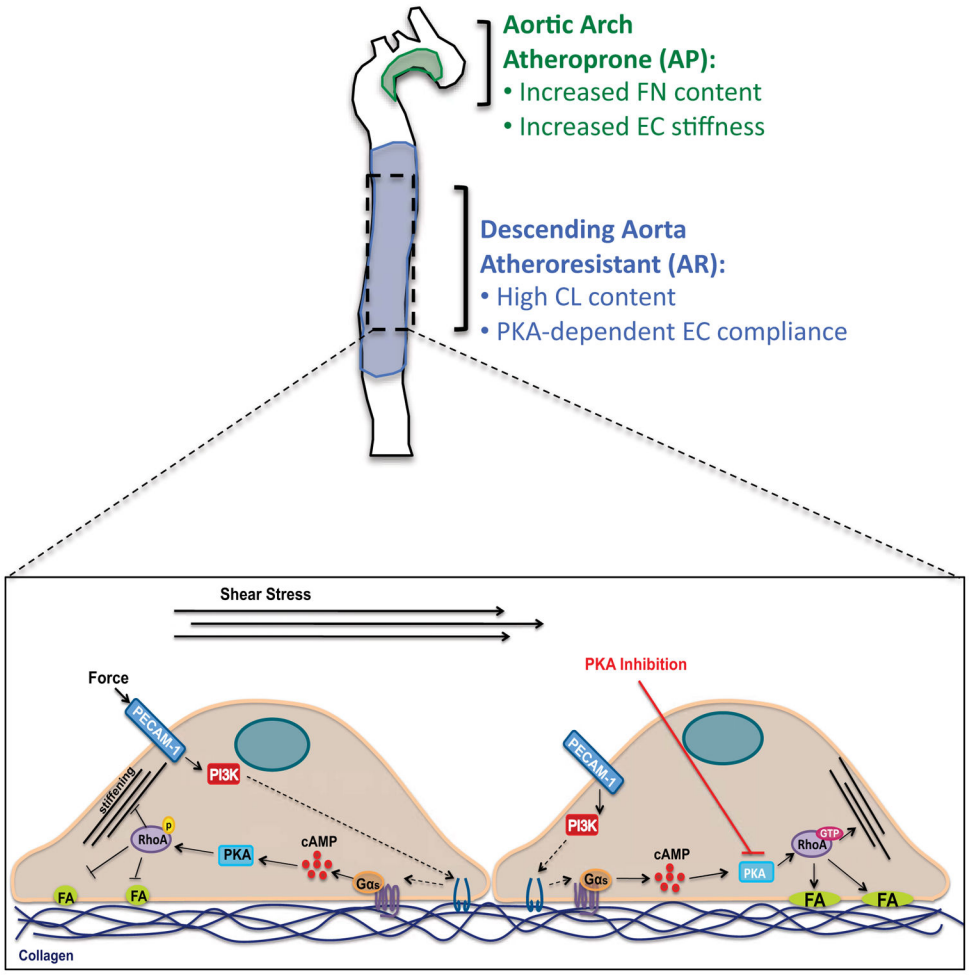

Figure 8. Model of CL-dependent PECAM-1 mechanosignaling

PECAM-1-dependent mechanosignaling through CL-binding integrins results in $G\alpha_s$-dependent PKA activation. PKA phosphorylates RhoA and inhibits its activity, which blunts EC stiffening responses. Inhibition of force-induced PKA activation promotes RhoA activation and is sufficient to restore the cellular response to force, including growth of focal adhesion and increased cellular stiffness.